The magnetic state of the low dimensional $CuTe_2O_5$ compound below 20 K

2008 J. Phys.: Condens. Matter 20 505210

(http://iopscience.iop.org/0953-8984/20/50/505210)

J. Phys.: Condens. Matter **20** (2008) 505210 (8pp) doi:10.1088/0953-8984/20/50/505210

The magnetic state of the low dimensional $CuTe_2O_5$ compound below 20 K

Marko Miljak[1,4], Mirta Herak[1], Ognjen Milat[1], Nenad Tomašić[2] and Helmuth Berger[3]

[1] Institute of Physics, POB-304, HR-10000 Zagreb, Croatia
[2] Institute of Mineralogy and Petrology, Horvatovac bb, HR-10000 Zagreb, Croatia
[3] Institute de Physique de la Matiére Complexe, EPFL, CH-1015 Lausanne, Switzerland

E-mail: miljak@ifs.hr

Received 20 June 2008, in final form 10 September 2008
Published 12 November 2008
Online at stacks.iop.org/JPhysCM/20/505210

Abstract
We report low field studies of the static magnetic susceptibility and torque measurements in the temperature range 2–330 K for the powder and crystalline $CuTe_2O_5$ compound. We show that the observed extraordinarily large magnetic axis rotation below 20 K and small (nearly negligible), but highly anisotropic, low temperature susceptibility upturn (which is thus of intrinsic nature) is a consequence of the changes within the ground state d^9 orbital doublet which take place below 20 K, smoothly.

1. Introduction

Magnetism of compounds relying on 3d transition metal ions reveals a wide variety of magnetic structures, magnetic dimensionalities and, accordingly, ground states. Underlying these varieties is the basic structural building block, a polyhedron formed of ligand ions (oxygen, sulfur, selenium etc) around the central 3d metal ion. In the crystal, ligand ions of polyhedra allow different ways of coupling neighboring central 3d magnetic moments and, together with the side-ions (cations), deliver magnetic systems spanning structural and magnetic dimensionalities from zero to three dimensions, with complex ground states. Because the symmetry of the electric field potential produced by the ligand ion charges determines the magnetic moment of the central 3d metal ion, its magnitude and the symmetry, it is clear that certain kinds of side-ions [1–3], as well as defects in the structure [4], may have profound effects on the resulting ground state.

The structure of $CuTe_2O_5$ is shown in figure 1. $CuTe_2O_5$ crystallizes in a monoclinic structure with space group $P21/c$, with lattice parameters $a = 6.871$ Å, $b = 9.322$ Å, $c = 7.602$ Å and $\beta = 109.08°$ [5]. The basic structural blocks are CuO_6 octahedra which form structural dimers through edge sharing of oxygens; see figure 1. Thus, provided that there is isotropic exchange interaction in the crystal, the weak anisotropy of the expected dimer-like spin susceptibility would simply reflect the anisotropy of the electron g-factor in accord with octahedral symmetry. The tellurium side-ion, Te^{4+}, in the structure takes positions between structural dimers, sharing oxygen ions with them; figure 1(b). Hence, the particular form of the temperature dependence of the susceptibility, like the susceptibility anisotropy, would depend on the variety of exchange coupling pathways between structural pairs of octahedra.

The overall temperature dependence of the magnetic susceptibility of the present $CuTe_2O_5$ compound reflects all characteristic features of dimerized (alternating) systems. At high temperatures, the susceptibility obeys the Curie–Weiss (CW) law, signifying antiferromagnetic coupling, passing through a broad maximum, χ^{max}, at around $T_{max} \approx 56.2$ K, and then decreases exponentially towards zero as the temperature decreases to zero, on account of the energy gap (figure 2).

At the lowest available temperatures (2 K) a small (nearly negligible) upturn shows up in the susceptibility, often assigned as indicating the presence of paramagnetic impurities or defects. However, such a small upturn greatly contradicts the experimentally obtained Curie constant reduced by 9%, which is usually accompanied by a proportionally large low temperature susceptibility upturn. It seems, thus, that the reduced Curie constant obtained from the high temperature CW plot may at least partially be reduced for reasons other than spins being missing from the majority spin assembly. Many models [6–9] were suggested for the magnetic behavior of chain-end spins, brought about by chain defects, accounting for the low temperature susceptibility

[4] Author to whom any correspondence should be addressed.

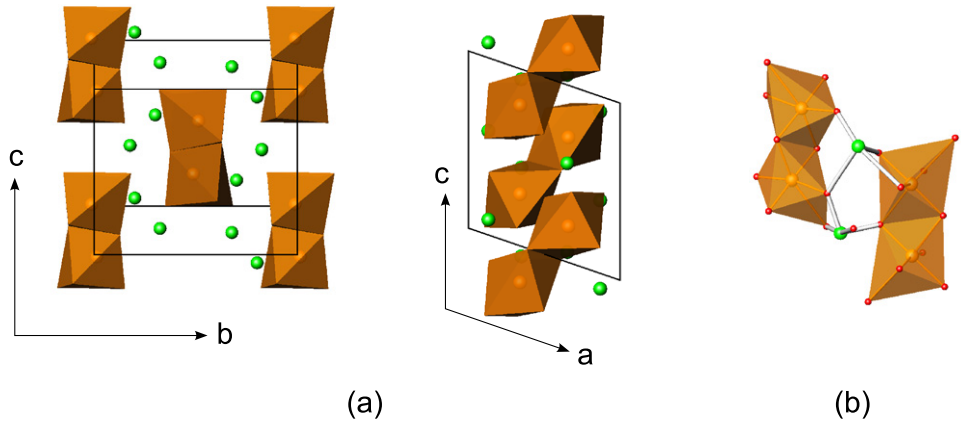

Figure 1. Crystal structure of $CuTe_2O_5$. (a) CuO_6 octahedra form structural dimers. Large spheres outside of the octahedra represent Te atoms. Oxygen atoms at the vertices of octahedra are not shown. Left: *bc* plane. Right: *ac* plane. (b) Two magnetically inequivalent pairs of CuO_6 octahedra in $CuTe_2O_5$. Tellurium ions form bonds (white) with oxygen ions.

(This figure is in colour only in the electronic version)

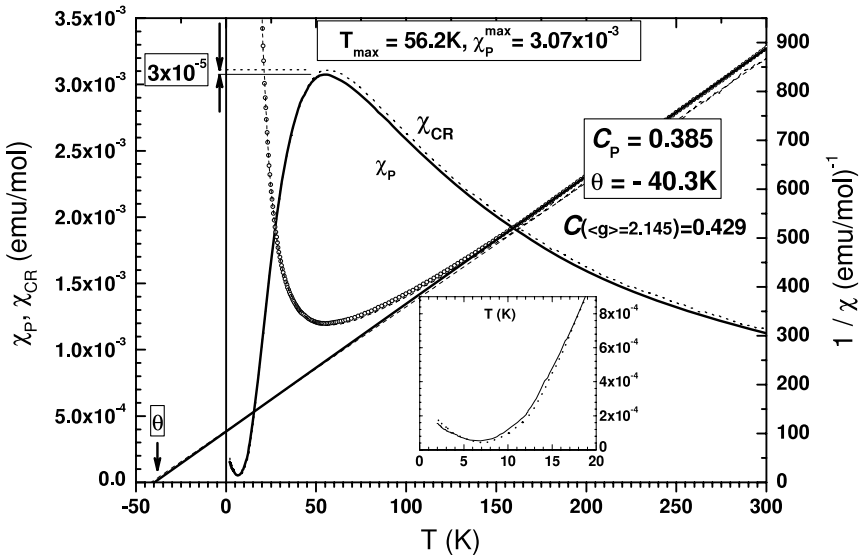

Figure 2. Temperature variation of the powder (solid line) and oriented crystal (dashed line) susceptibilities, left ordinate. CW plot of the powder and oriented crystal susceptibilities, right ordinate. The inset presents the low temperature part for both susceptibilities, powder and crystal.

upturn in regular and alternating low dimensional systems, whose resulting specific temperature dependences were experimentally proven [10, 11], even in some cases by susceptibility anisotropy measurements [12]. Considering the actual type of the low temperature divergence, it is closer to the CW law with weak ferromagnetic coupling than the fractional power law C/T^{ϵ} with $\epsilon < 1$ appropriate for alternating-chain assembly segmented randomly by defects [7, 9]. Moreover, detailed susceptibility anisotropy measurement by the torque method also reveals the low temperature upturn, which is surprisingly close in magnitude to the one in the susceptibility but, more importantly, reveals the large temperature dependent rotation of the magnetic axes. Summing up, from the low temperature susceptibility and susceptibility anisotropy features, there seems to be convincing evidence that the susceptibility upturn is intrinsic in origin. Adding temperature dependent rotation of magnetic axes to the latter summary, we have all the signatures that the ground state found for high temperatures (gapped, nonmagnetic) is modified below 20 K.

2. Experimental details

The Faraday force method, based on an electro-balance, was employed for static magnetic susceptibility measurement in the magnetic fields up to 9 kOe and the temperature region 2–330 K. The absolute accuracy of this method is well within 1%.

For measurements of the anisotropy of the susceptibility, we exploited a highly sensitive homemade torque magnetometer, in magnetic field up to 8 kOe and in the temperature region 2–330 K. The absolute accuracy is within 0.1%. The magnetometer is made of a thin and short (2 cm) quartz fiber

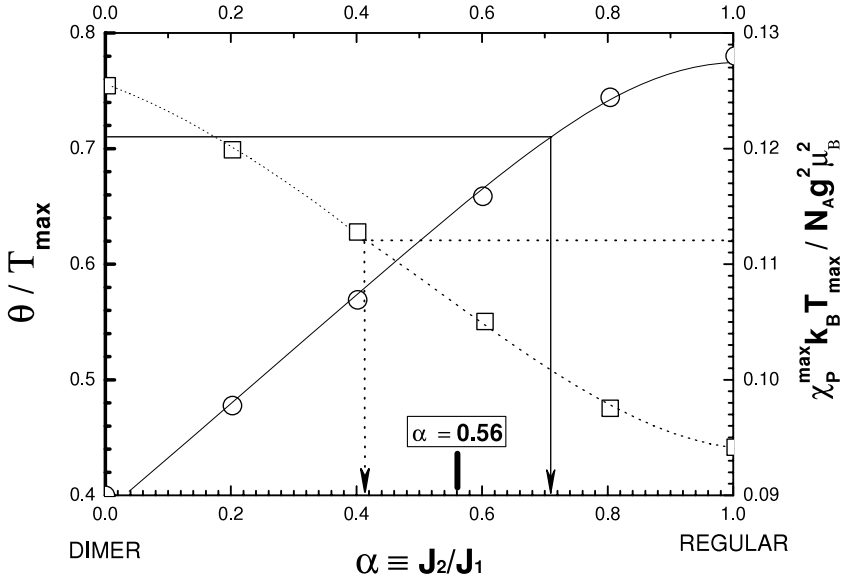

Figure 3. Experimental ratio $\Theta/T_{\max} = 0.71$ (left ordinate) and the product $\chi_P^{\max} k_B T_{\max}/4C_P = 0.112$ (right ordinate), versus chain alternation $\alpha = J_2/J_1$ where J_1 and J_2 are the nearest and next nearest neighbor exchange constants, respectively. For the spin $S = 1/2$, $N_A g^2 \mu_B^2/k_B = 4C_P$. α dependent square and circle values are given by [14].

with a small torsion constant ($k \approx 3 \times 10^{-3}$ erg rad^{-1}) fused to a thick and long (≈100 cm) quartz fiber. At the other end of the thick fiber the two quartz plates were fused in such a way as to allow sample mounting between them, without any glue. The fiber system hangs freely in the appropriate cryostat, while plates (sample) at the bottom of the thick fiber are situated in a homogeneous horizontal magnetic field, which can rotate by 360°. A small mirror at the top of the thick fiber serves for measuring the torsion angle of the tiny fiber and hence the magnetic torque exerted by the applied field, monitoring the mirror-reflected laser beam with a movable photo-diode.

3. Results

3.1. Magnetic susceptibility

Figure 2 presents raw (uncorrected) susceptibility data together with the CW plot for the powder (P) and oriented crystal (CR) samples. The lowest raw susceptibility value, centered at about 7 K (see inset of figure 2), presumably already in the gapped state, amounts to 4.5×10^{-5} emu mol^{-1}, and, together with the value of the temperature independent diamagnetic correction [13] of $\chi_{DIA} = -1.00 \times 10^{-4}$, suggests a Van Vleck orbital contribution of about $\langle\chi_{VV}\rangle = 1.45 \times 10^{-4}$ emu mol^{-1}, similar to the literature quoted values. It is noteworthy that above $T_{\max}$ the oriented crystal sample susceptibility lies above the powder susceptibility, while below 20 K (see the inset) it crosses smoothly below the powder susceptibility, indicating changes of magnetic symmetry below 20 K. Note that the Curie constant obtained from the CW plot (C_P, solid box) shows a reduction with respect to the calculated one, $C_{\langle g\rangle=2.145} = 0.429$ emu K mol^{-1}, of about 9%, assuming an average electron g-factor of $\langle g\rangle = 2.145$, reported frequently for Cu^{2+} based compounds. Thus, it is clear that fitting susceptibility data with any particular susceptibility model would demand the introduction of some parameters not definable by the present method, at least e.g. inter-chain coupling. In order to establish the type of the underlying magnetism, seemingly of importance considering a foregoing announcement of changes within ground state, we instead sum up below all necessary experimental parameters for a single route of model classification, exploiting the Duffy and Barr (DB) diagram [14] (inset of figure 12 of [14]), figure 3.

The parameters obtained from figure 2 are as follows: $\chi_P^{\max} = 3.07 \times 10^{-3}$ emu mol^{-1}, $\chi_{CR}^{\max} = 3.10 \times 10^{-3}$ emu mol^{-1} for powder and crystal respectively; $T_{\max} = (56.2 \pm 0.3)$ K for both samples; Curie constants $C_P = 0.385$ emu K mol^{-1} and $C_{CR} = 0.390$ emu K mol^{-1}; and the Weiss constant for both sample types $\Theta = -40.0 \pm 0.5$ K, thus signifying a moderate antiferromagnetic exchange constant, $J < 0$.

Using experimental values of $\chi_P^{\max}$, $T_{\max}$ and the Curie constant C_P, we obtain in figure 3 a point appropriate to the right ordinate, $\chi_P^{\max} k_B T_{\max}/4C_P$, of 0.112, corresponding to the alternation $\alpha \approx 0.41$ (dotted guideline). On the other hand, the ratio $\Theta/T_{\max} = 0.71$ appropriate to the left ordinate results in alternation $\alpha \approx 0.71$ (solid guideline). Though different, the values of the alternation prove nevertheless the features of alternating-chain assembly rather than of an isolated dimer system. Furthermore, the DB diagram offers straightforward guidance in the approach, making these two values of alternation coincide at $\alpha \approx 0.56$, close to the value of $J_1/J_6 = 0.59$ of [15], where J_1 corresponds to our J_2 and J_6 to our J_1. In other words, the only way to achieve the same value of α requires the assumption of the simultaneous presence of weak ferromagnetic inter-chain coupling that enhances $\chi_P^{\max}$ and weak frustration effects that enhance the ratio $\Theta/T_{\max}$. In comparison with strongly frustrated compounds with $\Theta/T_{\max} > 5$ [16], the present compound displays rather weak frustration effects. The

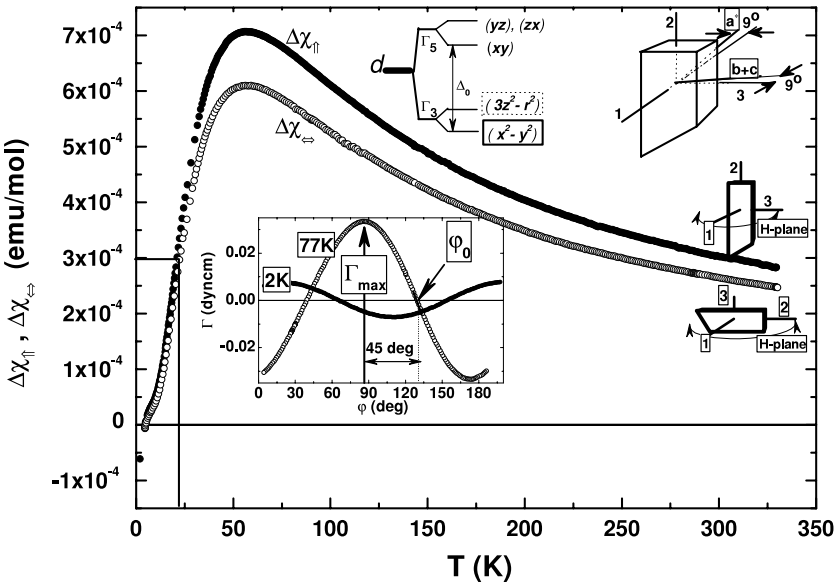

Figure 4. Temperature variation of the susceptibility anisotropies for two mutually orthogonal sample orientations, $\chi_{\Uparrow}$, $\chi_{\Leftrightarrow}$ (sketched close to the corresponding data set, including three mutually orthogonal verticals, 1, 2, 3, to the crystal facets). The top right drawing represents positions of the crystal axes, showing the deflection of a^* and $b+c$ axes by 9° in the 13 plane of the crystal. The top middle drawing presents the energy level scheme of the Cu^{2+} ion in the octahedral ligand surrounding with tetragonal distortion [19].

presence of frustration is indicated also by fitting susceptibility data to gapped susceptibility models [17, 18]. Considering thus the parameters obtained from high temperature susceptibility data, the present compound can be described as a weakly frustrated alternating-chain system with alternation $\alpha \approx 0.56$.

3.2. The susceptibility anisotropy

Note that in the absence of single-ion anisotropy energy (D), the weak susceptibility anisotropy of the 3d metal ions surrounded by the ligand ions is governed mainly by the effects of the crystal (ligand) field. Thus, the resultant magnitude of the magnetic moment and, particularly, the symmetry of its electron g-tensor that determine the susceptibility tensor can be suitably monitored by the torque methods. In the cases of paramagnetic and diamagnetic substances the measured torque resulting from the susceptibility anisotropy $\Delta\chi_{xy} \equiv (\chi_x - \chi_y)$, where x and y are mutually orthogonal magnetic axes in the field plane, defined by the vector product of the magnetic field and the magnetization, is given by

$$\boldsymbol{\Gamma} = V\mathbf{M}\times\mathbf{H} = V(M_x\hat{x}+M_y\hat{y}+M_z\hat{z})\times(H_x\hat{x}+H_y\hat{y}+H_z\hat{z}) \tag{1}$$

$$M_i = \sum_j \chi_{ij}H_j, \qquad \forall i, j = x, y, z$$

which reads

$$\Gamma_z = \frac{m}{2M_{\mathrm{mol}}}\Delta\chi_{xy}\sin(2\varphi - 2\varphi_0)H^2 \tag{2}$$

where m denotes the sample mass, M_{mol} represents the formula unit mass, H stands for the magnetic field strength, φ is the field goniometer angle, φ_0 is the angle at which the magnetic field points, in the direction of one of the magnetization axes in the xy plane, $\Delta\chi_{xy}$ is expressed in units of emu mol^{-1}. From (2) it is evident that when the field direction φ coincides with any of the magnetization axes ($M_{x,y,z}$) the torque takes the zero value, defining the experimental angle φ_0 that is the direction of the crystal magnetic axis which can be correlated with crystal axes if these are checked by x-ray analysis.

Experimentally, the temperature variation of the anisotropy reduces in simple cases to the measurement of the temperature dependence of the torque amplitude for the applied magnetic field in a fixed ($\varphi_0 \pm 45°$) direction, once φ_0 is determined at fixed temperature (inset of figure 4). However, in the general case, two independent anisotropic subsystems whose magnetic axes do not coincide result in superposition of anisotropies and the effective magnetic axis direction would vary with temperature. Nevertheless, there are other intrinsic causes for temperature variations of the magnetic axis directions in 3d metal ion based compounds, all causing changes in crystal field symmetry, for example the static Jahn–Teller effect, charge order etc. Hence, because any factor causing temperature variations of the magnetic axis direction, φ_0, may also cause changes of torque amplitude, there is clearly a need for simultaneous determination of these quantities. The requirement is accomplished experimentally by tracing a narrow ($\pm 2°$) linear portion of the torque sine curve in the vicinity of one of the zero crossings φ_0 (short line marked by an arrow in the inset of figure 4) for various fixed temperatures. Such a detailed torque procedure enables thus simultaneous determination of the resultant torque amplitude, i.e. the resultant or true anisotropy, and the actual magnetic axis direction (φ_0) at each temperature, as shown in figures 6(a) and (b) of section 4.

Figure 4 displays the temperature variation of the susceptibility anisotropies for two mutually orthogonal single-crystal orientations obtained by the standard procedure, i.e. by monitoring the temperature variation of the torque amplitude

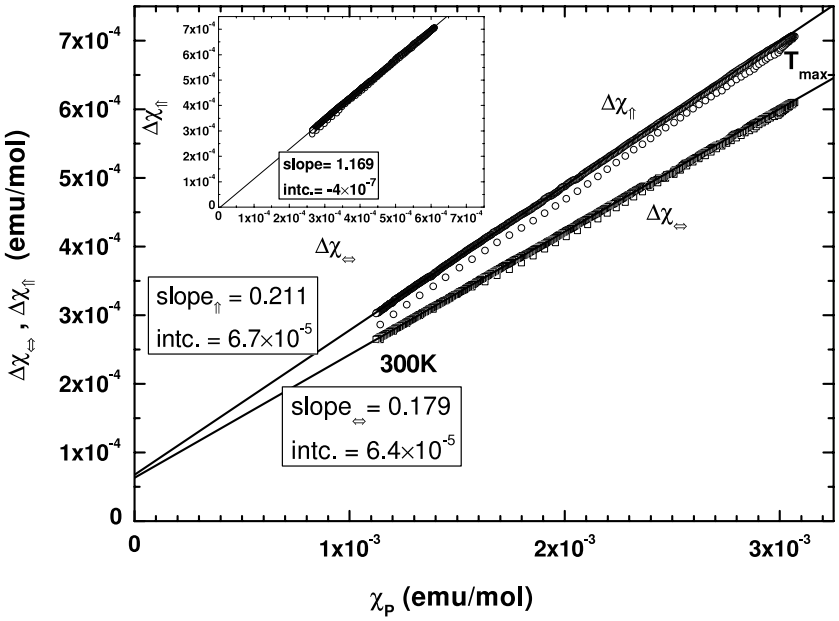

Figure 5. Correlation diagram of measured susceptibility anisotropies $\Delta\chi_{\Uparrow}$ and $\Delta\chi_{\Leftrightarrow}$ with raw powder susceptibility $\chi_{\rm P}$. Inset: correlation diagram of $\Delta\chi_{\Uparrow}$ with $\Delta\chi_{\Leftrightarrow}$.

($\Gamma_{\rm max}$ in the inset of figure 4) with the applied field direction at the fixed angle ($\varphi_0 + 45$ degrees; see the inset of figure 4). The inset of figure 4 shows the angular dependence of the torque measured at 77 and 2 K. Both curves are sine curves, in accord with (2), but differing in phase, clearly showing large change of the magnetic axis direction φ_0 at low temperatures. The figure supplies sketches of the crystal sample morphology and its orientation in the field (marked as the H plane) and drawings of some crystal axis directions as found by x-ray analysis.

4. Combined susceptibility and anisotropy data

The high temperature anisotropy data (above 20 K) closely follow the temperature dependence of the powder susceptibility $\chi_{\rm P}$ with proportionality adequate for an anisotropic temperature independent electron g-factor of the Cu^{2+} ion in an octahedral ligand surrounding, $\Delta\chi = \chi_{\rm P} \cdot [(g_1^2 - g_2^2)/\langle g\rangle^2]$. Another informative diagram, correlating anisotropy and susceptibility of powder $\chi_{\rm P} = (\chi_1 + \chi_2 + \chi_3)/3$ data, is shown for both crystal orientations, in figure 5.

The large range of linearity (from high temperature down to $T_{\rm max}$) in this correlation diagram for both crystal orientations proves that small anisotropy originates from anisotropy of the electron g-factor. In order to verify the consistency of the two kinds of data, the susceptibility and the anisotropy, particularly as regards absolute values, we present in the inset of figure 5 the correlation of two anisotropies, and compare the parameters obtained, the slope and intercept, with the corresponding parameters of the main correlation diagram. The slope of the inset diagram (framed text) agrees within 1% with the ratio of the corresponding slopes of the main diagram (framed text) verifying thus complete consistency, and providing the possibility of drawing some reliable conclusions as follows. Firstly, agreement of slopes undoubtedly verifies the underlying electron g-factor anisotropy, high absolute accuracies of both magnetic methods and coordination of their thermometry. Secondly, considering the intercepts in the inset and in the main correlation diagram, which are practically zero (inset of figure 5) and nearly equal for the two sample orientations (6.7×10^{-5} and 6.4×10^{-5} emu mol^{-1}, framed text) respectively, these practically identical values verify the presence of an anisotropic temperature independent orbital (Van Vleck) paramagnetic contribution. Accounting for the excess $\langle\chi_{\rm VV}\rangle = 4.5 \times 10^{-5}$ emu mol^{-1} over $\chi_{\rm DIA}$ at about 7 K (cf the inset of figure 2) we obtained upper bounds to $\Delta\chi_{\rm VV}$ of 7.8×10^{-5} and 7.2×10^{-5} emu mol^{-1} appropriate for Cu^{2+} ions in octahedral oxygen surroundings. Thirdly, the slopes of the main correlation diagram (framed text) agree with a number of published values of electron g-factor anisotropies for the Cu^{2+} ion in octahedral oxygen surroundings, and particularly with ESR data obtained for a crystal sample of the same chemical formula as the present compound [15].

Note that the difference in magnitude between the two anisotropies in the main diagram (figure 5) partially arises from the crystal a^* axis being deflected by about 9° from the largest sample facet, whose vertical (axis 1 in figure 4) represents the axis of rotation between two orthogonal crystal orientations, as checked by the x-ray examination. Note furthermore a slight departure from high temperature linearity in the main diagram (and less perceptibly in the inset) starting at maximal average susceptibility or, correspondingly, at $T_{\rm max}$. In these combined types of measurement the departure from linearity (or slight change in slope) is the manifestation of weak anisotropy of the antiferromagnetic exchange constant J, of about 1 K. The detected weak exchange anisotropy does not seriously alter the values of the anisotropic quantities evaluated at high temperatures. We cannot argue, however, that this anisotropy at $T \to 0$ K plays no role.

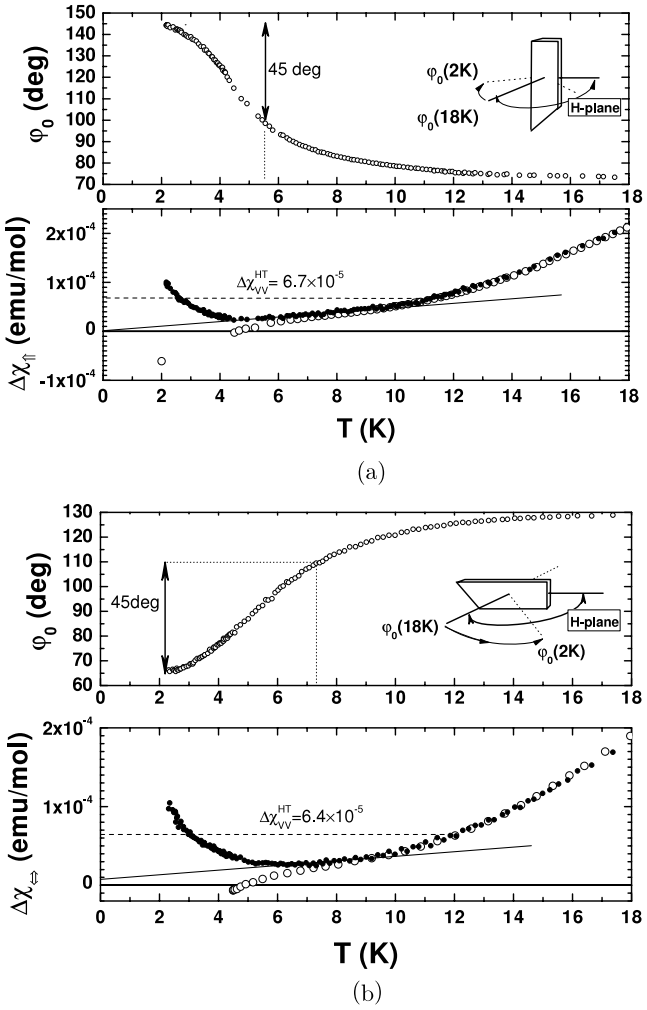

Figure 6. Temperature dependence of the magnetic axis position φ_0 (top panels of (a) and (b)) and susceptibility anisotropy obtained from two different sets of measurements, as described in the text (bottom panels of (a) and (b)). Full symbols represent true anisotropy and empty symbols anisotropy obtained by standard measurement. (a) and (b) correspond to results obtained for two mutually perpendicular planes of measurements. The H plane is the field plane.

Hence, both the g-factor and the orbital or Van Vleck paramagnetism of the magnetic moment of the Cu^{2+} ion possess nearly uniaxial symmetry, in accord with the octahedral oxygen surrounding. In other words, observation of a typical magnitude of the anisotropy of the Van Vleck orbital susceptibility proves that for $T > 20$ K the magnetic features of the present compound stem from the $d_{x^2-y^2}$ orbital state, shown by solid box in top middle energy level scheme [19] in figure 4.

While the conclusions just reached from susceptibility and anisotropy data at temperatures above 20 K clearly suggest a gapped and nonmagnetic ground state, the detailed torque measurements below 20 K suggest differently. Figure 6 displays true anisotropies obtained by the detailed torque procedure. Figures 6(a) and (b) correspond to two mutually orthogonal sample orientations. The top panel of each figure presents the temperature dependence of φ_0 and the bottom panel presents the true anisotropy (full symbols) and the anisotropy obtained by the standard procedure (empty symbols), added for comparison. The true anisotropy (full symbols) coincides above 20 K with anisotropies obtained by the standard measuring procedure (not shown). Comparison of anisotropies obtained by these two different procedures clearly shows that the opposite behavior at low T, upturn/downturn (cf figure 5 /figure 4), results from sliding of the torque sine curve or equivalently continuous sliding of φ_0 with temperature; these were not followed by the standard torque procedure.

As displayed in figure 6 (top panels), these detailed torque data prove rotation of the magnetic axes below 20 K by more than 60° for both sample orientations. These measurements ensure hence both the quantitative reliability of the anisotropy upturn and its form of temperature dependence. Most importantly, however, the measurements reveal the temperature variation of the anisotropy in the temperature region where the high temperature data suggest a gapped state with zero spin susceptibility and accordingly zero spin susceptibility anisotropy.

From the bottom panels of figures 6(a) and (b) we see that the finite value of the true anisotropy in the nonmagnetic low T state, which should correspond to the anisotropy of the temperature independent Van Vleck susceptibility, is 50% less than the value obtained from high T data, marked by dashed line. As seen for both sample orientations (bottom panels of figure 6), the reduction takes place below about 11 K, smoothly, and continues quasi-linearly down to about 5 K. If this quasi-linear reduction extrapolated to zero temperature (solid lines) it would result in a zero or vanishingly small intercept, i.e. a vanishingly small orbital Van Vleck susceptibility anisotropy, in contrast to the high temperature data, which are compatible with a $d_{x^2-y^2}$ orbital state. Conversely, a vanishingly small orbital Van Vleck susceptibility anisotropy is compatible with a $d_{3z^2-r^2}$ orbital state (marked by a dotted box in the energy scheme in figure 4).

The unusual temperature variation of the true anisotropy, which decreases with decreasing temperature between 10 and 4 K and sharply increases below 4 K, is not compatible with contributions of anisotropic paramagnetic impurities or defects which normally do not change the sign of the contribution with temperature. Similarly, the temperature variation of φ_0 data, where φ_0 changes by more than 50° below 10 K, cannot be explained by superposition of the two magnetic subsystems. This is because, in the most efficient circumstances of relative subsystem orientations of 45°, φ_0 can reach at most changes of 45.0°. Hence, these experimental findings undoubtedly reflect fundamental intrinsic symmetry changes and as such point to changes in quantities that are fundamentally dependent on local symmetry, i.e. in the present case to the changes of the orbital Van Vleck paramagnetic contribution. Hence, any reliable attempt at fitting a small low temperature upturn to the available established susceptibility laws, like the Curie, Curie–Weiss and C/T^{ϵ} power laws, is hindered by the uncertainty in the orbital Van Vleck contribution. In order to avoid the latter uncertainty and possibly anticipate the origin of the most intriguing anisotropy and susceptibility upturn developing

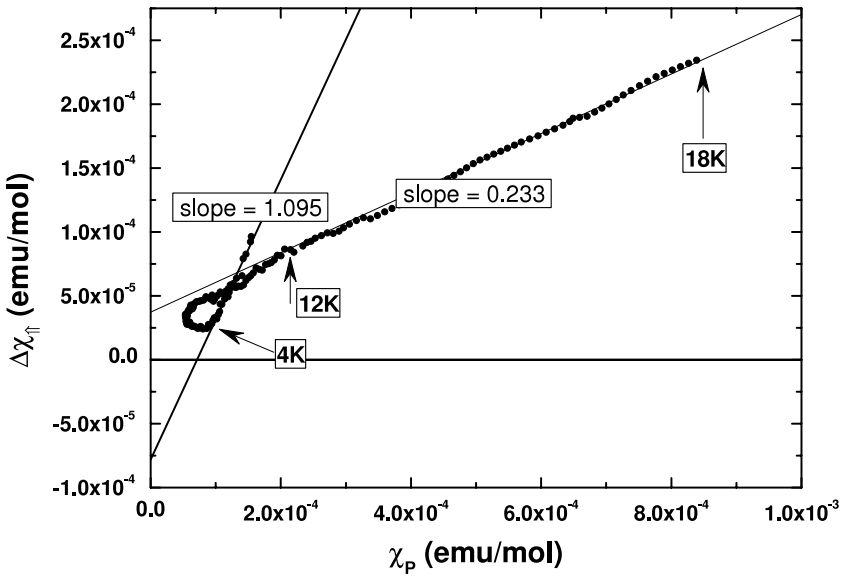

Figure 7. Low temperature correlation of the true anisotropy and powder susceptibility below 20 K.

below ≈5 K, we make a test using the correlation diagram for the true anisotropy and the susceptibility shown in figure 7. For the sake of clarity, in figure 7 we present only one true anisotropy data set, $\Delta\chi_{\Uparrow}$, versus powder susceptibility χ_{P}. The slope of the higher temperature region 18–12 K (solid box) in this diagram is somewhat larger than the declared high temperature slope (=0.211) of figure 5, showing actually continuation of the departure from linearity starting from $T_{\max}$ discussed above, in the description of figure 5. At temperatures below 5 K, the upturn displays an extraordinary large slope ≈1, overshooting the largest reported g-factor anisotropy (≈0.3), suggesting the appearance of another temperature dependent inherently anisotropic susceptibility contribution.

5. Discussion and conclusion

The central result, the anomalously large slope in figure 7 and, particularly, the large negative intercept, verifies the intrinsic nature of the upturn. This result hence serves to discriminate between various origins of the low temperature upturn relying on Cu^{2+} electron g-factor and its anisotropy, i.e. applications of all models that present circumstances like an interacting CW law, the one-dimensional diverging and power laws induced by defects [6, 7, 9], and also logarithmic divergence without defects [8]. This is because any (additive) upturn following the latter susceptibility laws should give an understandable intercept: zero or a small positive value in our case. It is more likely that the observed susceptibility upturn belongs to the other class of temperature dependent susceptibilities (exponential), that only mimic the above fundamental susceptibility laws, in a rather restricted temperature range in the present case.

As a suggestion, note that the large slope obtained, $\geqslant 1$, is comparable to the slopes observed in the case of antiferromagnetic ordering, slope $= (\chi_{\perp} - \chi_{\parallel})/(1/3(2\chi_{\perp} + \chi_{\parallel}))$, and also that the parallel susceptibility $\chi_{\parallel}$ vanishes below the ordering temperature towards $T = 0$ K as the singlet susceptibility does, i.e. in an exponential fashion. The intriguing ground state with high intrinsic susceptibility anisotropy at low temperatures may also correspond to the model which describes a gapless ground state of a linear antiferromagnetic chain under the staggered field induced by the applied field, wherein at low temperature it produces growing paramagnetic susceptibility similar to the impurity susceptibility, but highly field direction dependent [20]. In any case, attribution of the observed highly anisotropic susceptibility upturn to either weak antiferromagnetism [21, 22] or an intrinsic upturn caused by staggered fields [20] also pre-supposes ground states that are different from the simple gapped nonmagnetic one suggested from high temperature magnetic data. Besides, considering important experimental information on an undoubtedly gradual temperature variation of both the true anisotropies and φ_0 from 20 K down to about 5 K, any supposed influence on the Cu^{2+} ion should emerge in a smooth fashion too. The latter fact suggests that the possibility of any customary sole intrinsic cause like a structural transition, a static Jahn–Teller effect, charge ordering etc can be excluded, because these will all manifest in sharp (step-like) changes primarily of φ_0 but of the true anisotropy also. At present, considering the smooth influences on φ_0 and the true anisotropy, the only suggestion known to the authors considers the effect of the zero-point motion in the Jahn–Teller effect [19], i.e. admixture of $d_{x^2-y^2}$ and $d_{3z^2-r^2}$ orbital states. According however to another empirical notion of the effects of specific side-ions (the lone-pair ions: Tl^{+}, Ge^{2+}, Sn^{2+}, Pb^{2+}, As^{3+}, Sb^{3+}, Bi^{3+}, Se^{4+}, Te^{4+}, etc), because of their high polarizability and strong preference for unusual stereochemistry [2], the effects of lone-pair ions may also emerge in a smooth fashion.

The presence of the tellurium ion in the Te^{4+} ionic state in $CuTe_2O_5$ gives thus an indication of a possible origin of the unusual features presented. Note that similarly large magnetic axis rotations followed by measuring φ_0 were observed in the

$NiSeO_3$ compound [1], where selenium ions are in the Se^{4+} ionic state, which also has a lone electron pair.

We would like to stress the specific rare way of pairing oxygen octahedra in the present compound (sharing the edge of the triangular octahedron facet; see figure 1), which allows any distinct directional strain applied to the coupled octahedral pair unit to transmit along other directions in both octahedra of the pair. Hence, we may expect the appearance of both types of octahedral distortions, tetragonal and trigonal. Therefore we may expect effects on the splitting of the Γ_3 ground orbital doublet wherein the tetragonal distortion does split the orbital doublet while the trigonal distortion does not [19]. It is possible in the present case that the effects of Te^{4+} lone-pair ions realize (in the low temperature region) a moderate percentage of trigonal distortion, i.e. partial splitting of the Γ_3 orbital ground doublet, influencing the Van Vleck orbital susceptibility and accordingly its anisotropy.

Furthermore, the high polarizability of Te^{4+} ions [2] and possible dipolar ordering may affect φ_0 in a smooth fashion. A smooth change of φ_0 has been observed in the $(TMTSF)_2FSO_3$ organic two-chain compound [23], where small electric dipoles exist on asymmetric FSO_3 anions. Electric dipolar ordering would add an electric field potential and symmetry to the otherwise purely ionic octahedral crystal field on the Cu^{2+} ion. On specific occasions when an inversion center for the 3d ion is lacking (e.g. because of Te^{4+} activity), the combined effect of an electric and a magnetic field may cause splitting of the ESR lines [19].

We would like to emphasize finally that whatever the intrinsic cause for the observed magnetic axis rotation, it is not without effect on magnetic quantities used for ground state determination, like exchange coupling constants J_1 and J_2, alternation α, Weiss constant Θ and, accordingly, local symmetry changes which allow Dzyaloshinskii–Moriya interaction to enter etc. Thus, alternating-chain features (alternation α) observed at high temperatures as well as the dimensionality may be changed at low temperatures via the Te^{4+} ion influence. As a consequence, various ground states and quantum criticalities are possible.

In summary, the high temperature state above 20 K is fully compatible with the $d_{x^2-y^2}$ orbital state of the Γ_3 doublet (marked by a solid box in the crystal field energy level scheme in figure 4) while the orbital state compatible with the vanishing orbital Van Vleck susceptibility, evidenced in the temperature range 12–5 K, should have an admixture of the $d_{3z^2-r^2}$ orbital state (marked by the dotted box in the level scheme). In conclusion, the unusually strong anisotropy (far beyond the electron g-factor anisotropy) of the small low temperature susceptibility upturn, emphasizing its intrinsic nature, serves to provide an indication of the changes within the ground state d^9 orbital doublet below 20 K, but also locates the present compound in the rich field of symmetry-broken states, and the competition between different types of order and interaction in insulating quantum spin systems.

Acknowledgments

MM and MH gratefully acknowledge the support of the Swiss National Science Foundation SCOPES project *Sparsely connected antiferromagnets: ground states, clusters and domains* (No. IB7320-111105) and the Croatian Ministry of Science, Education and Sports under Grant No. 035-0352843-2846.

References

[1] Miljak M, Becker R, Herak M, Prester M, Milat O, Johnsson M and Berger H 2007 *J. Phys.: Condens. Matter* **19** 196203
[2] Kohn K, Inoue K, Horie O and Akimoto S 1976 *J. Solid State Chem.* **18** 27
[3] Geertsma W and Khomskii D 1996 *Phys. Rev.* B **54** 3011
[4] Uchinokura K 2002 *J. Phys.: Condens. Matter* **14** R195
[5] Hanke K, Kupcik V and Lindqvist O 1973 *Acta Crystallogr.* B **29** 963
[6] Bonner J C and Fisher M E 1964 *Phys. Rev.* **135** A640
[7] Bulaevsky L N, Schegolev I F, Zvarykin A V, Lyubovsky R B and Karimov Y S 1972 *Sov. Phys.—JETP* **62** 725
[8] Fujimoto S and Eggert S 2004 *Phys. Rev. Lett.* **92** 037206
[9] Fisher D S 1995 *Phys. Rev.* B **51** 6411
[10] Miljak M, Korin B, Cooper J R, Holcyer K, Grüner G and Janossy A 1980 *J. Magn. Magn. Mater.* **15–18** 219
[11] Cooper J R, Miljak M and Korin B 1980 *Chem. Scr.* **17** 79
[12] Miljak M, Herak M, Revcolevschi A and Dhalenne G 2005 *Europhys. Lett.* **70** 369
[13] Selwood P W 1956 *Magnetochemistry* 2nd edn (New York: Interscience)
[14] Duffy W and Barr K P 1968 *Phys. Rev.* **165** 647
[15] Deisenhofer J, Eremina R M, Pimenov A, Gavrilova T, Berger H, Johnsson M, Lemmens P, von Nidda H A K, Loidl A, Lee K S and Whangbo M H 2006 *Phys. Rev.* B **74** 174421
[16] Miyahara S and Ueda K 1999 *Phys. Rev. Lett.* **82** 3701
[17] Bulaevskii L N 1969 *Sov. Phys.—Solid State* **11** 921
[18] Troyer M, Tsunetsugu H and Würtz D 1994 *Phys. Rev.* B **50** 13515
[19] Abragam A and Bleaney B 1970 *Electronic Paramagnetic Resonance* (Oxford: Clarendon)
[20] Affleck I and and Oshikawa M 1999 *Phys. Rev.* B **60** 1038
[21] Kotov V N, Zhitomirsky M E, Elhajal M and Mila F 2004 *Phys. Rev.* B **70** 214401
[22] Takagi R, Johnsson M, Gnezdilov V, Kremer R K, Brenig W and Lemmens P 2006 *Phys. Rev.* B **74** 014413
[23] Miljak M, Cooper J R and Bechgaard K 1988 *Phys. Rev.* B **37** 4970